Generation and coherent control of pulsed quantum frequency combs

Article (Published Version)

Video Article

Generation and Coherent Control of Pulsed Quantum Frequency Combs

Benjamin MacLellan*[1], Piotr Roztocki*[1], Michael Kues[1,2], Christian Reimer[1], Luis Romero Cortés[1], Yanbing Zhang[1], Stefania Sciara[1,3], Benjamin Wetzel[1,4], Alfonso Cino[3], Sai T. Chu[5], Brent E. Little[6], David J. Moss[7], Lucia Caspani[8], José Azaña[1], Roberto Morandotti[1,9,10]

[1]Institut National de la Recherche Scientifique - Centre Énergie, Matériaux et Télécommunications (INRS-EMT)

[2]School of Engineering, University of Glasgow

[3]Department of Energy, Information Engineering and Mathematical Models, University of Palermo

[4]School of Mathematical and Physical Sciences, University of Sussex

[5]Department of Physics and Material Science, City University of Hong Kong

[6]State Key Laboratory of Transient Optics and Photonics, Xi'an Institute of Optics and Precision Mechanics, Chinese Academy of Science

[7]Centre for Micro Photonics, Swinburne University of Technology

[8]Institute of Photonics, Department of Physics, University of Strathclyde

[9]Institute of Fundamental and Frontier Sciences, University of Electronic Science and Technology of China

[10]National Research University of Information Technologies, Mechanics and Optics

*These authors contributed equally

Correspondence to: Michael Kues at michael.kues@emt.inrs.ca, Roberto Morandotti at morandotti@emt.inrs.ca

URL: https://www.jove.com/video/57517
DOI: doi:10.3791/57517

Keywords: Engineering, Issue 136, Quantum optics, integrated photonic devices, mode-locked lasers, nonlinear optics, four-wave mixing, frequency combs, high-dimensional states

Date Published: 6/8/2018

Citation: MacLellan, B., Roztocki, P., Kues, M., Reimer, C., Romero Cortés, L., Zhang, Y., Sciara, S., Wetzel, B., Cino, A., Chu, S.T., Little, B.E., Moss, D.J., Caspani, L., Azaña, J., Morandotti, R. Generation and Coherent Control of Pulsed Quantum Frequency Combs. *J. Vis. Exp.* (136), e57517, doi:10.3791/57517 (2018).

Abstract

We present a method for the generation and coherent manipulation of pulsed quantum frequency combs. Until now, methods of preparing high-dimensional states on-chip in a practical way have remained elusive due to the increasing complexity of the quantum circuitry needed to prepare and process such states. Here, we outline how high-dimensional, frequency-bin entangled, two-photon states can be generated at a stable, high generation rate by using a nested-cavity, actively mode-locked excitation of a nonlinear micro-cavity. This technique is used to produce pulsed quantum frequency combs. Moreover, we present how the quantum states can be coherently manipulated using standard telecommunications components such as programmable filters and electro-optic modulators. In particular, we show in detail how to accomplish state characterization measurements such as density matrix reconstruction, coincidence detection, and single photon spectrum determination. The presented methods form an accessible, reconfigurable, and scalable foundation for complex high-dimensional state preparation and manipulation protocols in the frequency domain.

Video Link

The video component of this article can be found at https://www.jove.com/video/57517/

Introduction

The control of quantum phenomena opens the possibility for new applications in fields as diverse as secure quantum communications[1], powerful quantum information processing[2], and quantum sensing[3]. While a variety of physical platforms are actively being researched for the realizations of quantum technologies[4], optical quantum states are important candidates as they can exhibit long coherence times and stability from external noise, excellent transmission properties, as well as compatibility with existing telecommunications and silicon chip (CMOS) technologies.

Towards fully realizing the potential of photons for quantum technologies, state complexity and information content can be increased through the use of multiple entangled parties and/or high-dimensionality. However, the on-chip generation of such optical states lacks practicality as setups are complicated, not perfectly scalable, and/or use highly-specialized components. Specifically, high-dimensional path-entanglement requires D coherently-excited identical sources and elaborate circuits of beam-splitters[5] (where D is the state dimensionality), while time-entanglement needs complex multi-arm interferometers[6]. Remarkably, the frequency-domain is well-suited for the scalable generation and control of complex states, as shown by its recent exploitation in quantum frequency combs (QFC)[7,8] using a combination of integrated optics and telecommunication infrastructures[9], and provides a promising framework for future quantum information technologies.

On-chip QFCs are generated using nonlinear optical effects in integrated micro-cavities. Using such a nonlinear micro-resonator, two entangled photons (noted as signal and idler) are produced by spontaneous four-wave mixing, via the annihilation of two excitation photons - with the resultant pair generated in a superposition of the cavity's evenly-spaced resonant frequency modes (**Figure 1**). If there is coherence between the

individual frequency modes, a frequency-bin entangled state is formed[10], which is often referred to as a mode-locked two photon state[11]. This state wave-function can be described by,

$$|\psi\rangle = \sum_{k=1}^{D} c_k |k_i, k_s\rangle, \text{ where } \sum |c_k|^2 = 1$$

Here, k_i and k_s are the single-frequency-mode idler and signal components, respectively, and c_k is the probability amplitude for the k-th signal-idler mode pair.

Previous demonstrations of on-chip QFCs highlight their versatility as viable quantum information platforms, and include combs of correlated photons[12], cross-polarized photons[13], entangled photons[14,15,16], multi-photon states[15], and frequency-bin entangled states[9,17]. Here, we provide a detailed overview of the QFC platform and a protocol for high-dimensional frequency-bin entangled optical state generation and control.

Future quantum applications, especially those to be interfaced with high-speed electronics (for timely information processing), demand the high-rate generation of high-purity photon states in a compact and stable setup. We use an actively mode-locked, nested cavity scheme to produce QFCs within the telecommunications S, C, and L frequency bands. A micro-ring is incorporated into a larger pulsed laser cavity, with optical gain (provided by an erbium-doped fiber amplifier, EDFA) filtered to match the micro-ring excitation bandwidth[18]. Mode-locking is actively realized via electro-optic modulation of the cavity losses[19]. An isolator ensures that pulse propagation follows a single direction. The resulting pulse train has very low root mean square (RMS) noise and exhibits tunable repetition rates and pulse powers. A high isolation notch filter separates the emitted QFC photons from the excitation field. These single photons are then guided through fibers for control and detection.

Our scheme is a step towards a high generation-rate, small-footprint QFC source, as all components used can potentially be integrated onto a photonic chip. Additionally, pulsed excitation is particularly well-suited for quantum applications. First, looking at a pair of micro-cavity resonances symmetric to the excitation, it generates two-photon states where each photon is characterized by a single-frequency mode– central for linear optical quantum computing[20]. As well, multi-photon states can be generated by moving to higher power excitation regimes and selecting multiple signal-idler pairs[15]. Second, as photons are emitted in known time windows corresponding to the pulsed excitation, post-processing and gating can be implemented to improve state detection. Perhaps most significantly, our scheme supports high generation rates of photon states using harmonic mode-locking without reducing the coincidence-to-accidental ratio (CAR) – which could pave the way for high-speed, multi-channel quantum information technologies.

To demonstrate the impact and feasibility of the frequency-domain, control of QFC states must be accomplished in targeted ways, ensuring highly efficient transformations and state coherence. To satisfy such requirements, we use cascaded programmable filters and phase modulators – established components in the telecommunications industry. Programmable filters can be used to impose an arbitrary spectral amplitude and phase mask on the single photons, with a resolution sufficient to address each frequency mode individually; and electro-optic phase modulators driven by radio-frequency (RF) signal generators facilitate the mixing of frequency components[21].

The most important aspect of this control scheme is that it operates on all quantum modes of the photons simultaneously in a single spatial mode, using single control elements. Increasing the quantum state dimensionality will not lead to an increase in the setup complexity, in contrast to path- or time-bin entanglement schemes. As well, all components are externally reconfigurable (meaning the operations can be altered without amending the setup) and use existing telecommunications infrastructure. Thus, existing and upcoming developments in the field of ultrafast optical processing can be directly transferred to the scalable control of quantum states in the future.

In summary, the exploitation of the frequency-domain by QFCs supports the high-rate generation of complex quantum states and their control, and, is thus well-suited for the harnessing of complex states towards practical and scalable quantum technologies.

Protocol

1. Generation of the High-dimensional Frequency-bin Entangled States via Pulsed Excitation

1. Following the scheme outlined in **Figure 2** (Generation stage), connect each component using polarization-maintaining optical fibers (for improved environmental stability).
2. Connect a power supply to the electro-optic amplitude modulator and apply a DC voltage offset, tuning the offset value until the optical power transmitted through it is approximately halved (measured using an optical power meter), *e.g.*, such that a peak transmission value of 2 mW is halved to 1 mW.
3. Measure the approximate external cavity length. Calculate the external cavity mode spacing using the relationship,

   $$\Delta\nu_{\text{ext}} = \frac{c}{n_{\text{eff}} L}$$

   where $\Delta\nu_{\text{ext}}$ is the external cavity mode spacing, *c* is the speed of light in vacuum, n_{eff} is the effective index of the cavity medium, and *L* is the external cavity length. For example, for a 20 m cavity comprised of fiber with an effective refractive index of 1.46, the approximate cavity mode spacing would be 10.2 MHz.
4. Turn on the EDFA to initiate lasing.
5. Insert the fast photodiode into the setup at either the cavity coupler or other ring ports. Connect the photodiode signal to an oscilloscope to observe the excitation field's intensity in the time-domain.
6. Set the oscilloscope time resolution to <100 ps (through the horizontal scale knob) in order to resolve the ns-scale pulses. At this step, without the modulator activated, the output on the oscilloscope will show unstable pulse operation with a low quality, high noise pulse train.

7. Connect a function generator to the electro-optic amplitude modulator. Set the frequency of the function generator output to the (approximate) external cavity mode spacing found above (or a harmonic of it). This signal performs the mode-locking. Choose either a pulse (rectangular) waveform or sine wave for amplitude modulation. Turn on the function generator.
8. Tune the RF function generator frequency and DC offset to optimize and stabilize the pulse train shape on the oscilloscope. If a pulsed driving signal is used, optimize its duty cycle.
9. Manually adjust the EDFA gain to reduce (or increase) pulse intensity to the regime where the properties of the generated photons are as desired by the user (CAR is a useful metric here - see below for details on its measurement). For this, compare the respective coincidence histograms generated by the visual interface that comes with the timing electronics.
10. Feed the timing electronics sync channel with the pulse train signal (detected by the photodiode) or the RF mode-locking signal to synchronize the single photon detectors with the photon pair generation.
11. To increase the generation rate of the QFCs, drive the mode-locking modulator at higher harmonics of the external cavity frequency spacing while simultaneously augmenting the EDFA gain to ensure the same power per pulse — this maintains the photon pair CAR while boosting the pair production rate (**Figure 3**). For this, increase the function generator output frequency and EDFA gain respectively.

2. Control of the High-dimensional Frequency-bin Entangled States

1. Following the scheme outlined in **Figure 2** (Control stage), connect all components using polarization-maintaining fibers. Beginning from the notch filter in the generation scheme, connect in series the first programmable filter, phase modulator, and second programmable filter. Finally connect the single photon detectors for measurement purposes.
2. **Programmable filter operation**
   NOTE: Depending on the specific application/measurement being performed, the control parameters of the QFC will vary and the phase and amplitude masks applied to the frequency modes must be determined accordingly. The amplitude mask can be used to attenuate or block certain frequency modes and the phase mask can impart an arbitrary phase shift on each mode.
   1. Determine the necessary masks for the desired application/measurement.
   2. Via the programmable filter visual interface[22], set the amplitude of the desired frequency mode channels and attenuate all others.
   3. Similarly, apply the phase mask (the phase applied to the undesired channels is unimportant, as they are fully attenuated). Control the programmable filter with a visual interface where the desired frequencies are selected.

3. **Phase modulation operation**
   1. Using phase modulation, driven by a periodic signal, split each spectral component into side-bands evenly spaced by the frequency of the signal generator that is driving the phase modulator. Use this to mix several different quantum frequency modes, analogous with spatial beam-splitters in path-entanglement schemes. In the quantum regime, electro-optic phase modulation is considered a quantum scattering operation[23].
   2. Determine the target frequency modes (dependent on D and the measurement/processing being performed) and calculate the voltage pattern (frequency and amplitude for a sine wave generator) to optimize the desired c_n values (see below for some details on this).
   3. Connect the signal generator to the RF amplifier using low-loss cables (such as SMC cables). Connect the RF amplifier output to the phase modulator, also using adequate RF cables. Once all RF ends are connected and properly terminated, bias the RF amplifier.
   4. Ensure that the RF amplifier has sufficient output power to drive the electro-optic phase modulator with sufficient voltage to meet the desired mixing conditions — these are on the order of several V_π (the half-wave voltage of the phase modulator). Also, ensure that the RF cables and connectors are adequate for the bandwidth and frequency range of the driving signal.
   5. Set the RF signal generator (which is driving the phase modulator) at a frequency which will overlap the desired modes with the created side-bands (*e.g.*, 33 GHz).
   6. Turn on the signal generator to mix the frequency modes.
   7. To verify that the correct modulation is applied, send a continuous-wave laser through the phase modulator and check that the output spectrum corresponds to the intended modulation using an optical spectrum analyzer (the modulation parameters can be further optimized, see notes).
      NOTE: Optimizing the mixing of frequency modes (determining the optimal function frequency and amplitude) is highly dependent on the desired mixing scheme, experiment being performed, and state dimensionality D. If possible, the mixing schemes should mix modes close to the initial frequency mode (at low-integer sidebands) to increase the mixing efficiency. For example, if $D = 2$, the mixing is recommended to occur halfway between the two frequency modes (thus, the phase modulation should be driven at a frequency which has an integer multiple equal to *half* the quantum mode frequency spacing, or free spectral range (FSR)). However, for $D = 3$, mixing is recommended to occur in the center frequency mode (phase modulation should be driven at a frequency with an integer multiple equal to the FSR). For example, with $D = 3$ and micro-cavity $FSR = 200$ GHz, the phase modulation driving signal is set to 33.33 GHz such that the $n = 6$ sideband overlaps with the neighboring frequency modes - while also leaving sufficient intensity in the center frequency mode. This results in the overlapping of sidebands neighboring modes $|k-1\rangle$, $|k\rangle$ and $|k+1\rangle$ at the center frequency mode $|k\rangle$. **Figure 4a** visualizes an example of the modulation process and the sideband coefficients. Each frequency mode undergoes the same phase modulation and creates the same sideband distribution, but centered about the original frequency mode (**Figure 4a**). For a single frequency mode, the sideband amplitudes are calculated as the coefficients of a Fourier series[24],

$$c_n = \nu_{\mathrm{m}} \int_0^{1/\nu_m} e^{i(\varphi_m(t) - n\theta)} dt$$

where c_n is the amplitude transferred to the n-th sideband, ν_{m} is the frequency that the phase modulator is driven at, $\varphi_{\mathrm{m}}(t)$ is the phase modulation pattern (periodic with frequency ν_{m}), and θ is the argument of the periodic modulation function ($\theta = 2\pi\nu_{\mathrm{m}} t + \phi$). For a sinusoidal driving signal, $\varphi_m(t) = M\sin(2\pi\nu_m t + \phi)$, the side-band amplitudes are described by the Jacobi-Anger expansion,

$$c_n = \nu_m \int_0^{1/\nu_m} e^{i(Msin(2\pi\nu_m t+\phi)-n(2\pi\nu_m t-\phi))}$$
$$= i^n J_n(M) e^{in\phi} e^{i2\pi n\nu_m t}$$

where $J_n(M)$ is the n-th order Bessel function of the first kind evaluated at M and $M = \pi V/V_\pi$ is the maximum phase shift (where V is the voltage amplitude of the single-tone driving signal).

3. Processing of the High-dimensional Frequency-bin Entangled States

1. **Single photon spectrum**
    1. Insert a single photon detector following the filtering of the excitation field from the QFC, at the output of a programmable filter.
    2. Via the programmable filter computer software, sweep over the full programmable filter bandwidth using a narrow bandpass filter amplitude mask, measuring photon count rates as a function of frequency. For example, if a visual interface/control script in MATLAB is used (that is interfaced with the programmable filter control and timing electronics), enter the desired filter bandwidth values and step number and click "Run". Ensure sufficient integration time to get proper photon counts.
    3. To reconstruct the spectrum from this data, plot (for example, using a Matlab script) the photon count rates against the corresponding wavelength (bandpass filter center) where they were acquired.

2. **Coincidence measurement**
    1. To perform a coincidence measurement, split and route the signal and idler photons to separate single photon detectors. If the programmable filter has multiple ports, use it to perform the separation. Otherwise, insert a dense-wavelength division multiplexer (DWDM) prior to the single photon detectors and use this to route the photons.
    2. Select a signal and idler pair (for example, the second resonance lines with respect to the excitation frequency, signal-2 and idler-2) using the programmable filter (via the supplied software interface) and route them to two separate single photon detectors. For example, for the WaveManager software, click the Flexgrid sub-menu, click "Add" and enter the wavelength and output port for the chosen channel[22].
    3. Record the arrival time of the signal and idler photons using the time-to-digital converter. From these measurements, compute the time delay between the two photons. Plot a histogram (for example, using a Matlab script) of coincidence counts for a time-delay τ between signal and idler — this provides a coincidence measurement.
    NOTE: The CAR metric compares the number of true coincidence counts from the generated photon pairs with the accidental coincidence counts arising from multi-photon processes and dark counts.
    4. From the above-computed measurement, record the number of counts in the center peak (coincidences stemming from photons produced in the same pulse, centered around the zero delay, $\tau = 0$) — which is the coincidence value.
    5. Record the average number of counts in each side-peak (coincidences of photons produced in different pulses, where τ is a multiple of the pulse train period, *i.e.*, the inverse of the pulse repetition rate), which is the accidental value.
    NOTE: The CAR is simply the ratio of these two values (coincidence value/accidental value).

3. **Density matrix reconstruction**
NOTE: The process for density matrix reconstruction depends on several parameters of the quantum state: the dimensionality of the photons, the number of photons, and which modes are being measured. The number of raw measurements required is equal to D^{2N}, where D is the dimensionality and N is the number of photons. So, for example, a two-photon pair with a dimensionality of $D = 3$ will require 81 measurements. This protocol will outline the general process for density matrix reconstruction, with examples for a pair of $D = 3$ frequency mode photons.
    1. Determine a set of basis vectors for the desired state and a set of projection vectors (see below for details on how to appropriately choose these).
    2. With a coincidence measurement, use either a programmable filter or a DWDM route signal and idler photons to separate single photon detectors.
    3. Via the programmable filter software control, select the desired frequency modes and attenuate all others. Set the phase mask values to realize each projection wavevector individually and record a coincidence measurement. It is important to allow the same integration time between different projection coincidence counts.
    4. Using a custom computer script, compute the density matrix of the photons using the raw coincidence count measurements of each projection wavevector (see below for relevant computational details).
    NOTE: When determining basis vectors for the density matrix measurement, they must span the state space. For the example case, the basis vectors are

$$B = \begin{pmatrix} |\bar{k},\bar{k}\rangle \\ |\bar{k},\bar{k}+1\rangle \\ |\bar{k},\bar{k}+2\rangle \\ |\bar{k}+1,\bar{k}\rangle \\ |\bar{k}+1,\bar{k}+1\rangle \\ |\bar{k}+1,\bar{k}+2\rangle \\ |\bar{k}+2,\bar{k}\rangle \\ |\bar{k}+2,\bar{k}+1\rangle \\ |\bar{k}+2,\bar{k}+2\rangle \end{pmatrix}$$

For a state $|\psi\rangle$, the density matrix describes the quantum state by,

$$\rho = |\psi\rangle\langle\psi|$$

The density matrix for any real physical system must be a positive-definite, Hermitian matrix - but due to noise, this may not always be the case. In the example case with the chosen basis, the wavevector for the ideal maximally frequency-entangled state can be represented as

$$|\psi\rangle = \frac{1}{\sqrt{3}}(|k,k\rangle + |k+1,k+1\rangle + |k+2,k+2\rangle)$$

and thus, the theoretical density matrix would be:

$$\rho_{th} = \frac{1}{3}\begin{pmatrix} 1 & 0 & 0 & 0 & 1 & 0 & 0 & 0 & 1 \\ 0 & 0 & 0 & 0 & 0 & 0 & 0 & 0 & 0 \\ 0 & 0 & 0 & 0 & 0 & 0 & 0 & 0 & 0 \\ 0 & 0 & 0 & 0 & 0 & 0 & 0 & 0 & 0 \\ 1 & 0 & 0 & 0 & 1 & 0 & 0 & 0 & 1 \\ 0 & 0 & 0 & 0 & 0 & 0 & 0 & 0 & 0 \\ 0 & 0 & 0 & 0 & 0 & 0 & 0 & 0 & 0 \\ 0 & 0 & 0 & 0 & 0 & 0 & 0 & 0 & 0 \\ 1 & 0 & 0 & 0 & 1 & 0 & 0 & 0 & 1 \end{pmatrix}$$

Projection measurements are taken on a series of projection wavevectors, $|\psi_v\rangle$. Coincidence counts for each projection are given as,

$$N_v = C\langle\psi_v|\rho|\psi_v\rangle$$

where C is a constant (see below for definition).

5. Choose an orthogonal set of $D^N \times D^N$, normalized matrices, $\{\Gamma_i\}$, such that

$$Tr(\Gamma_x\Gamma_y) = \delta_{x,y}$$

where Tr is the trace, D is the dimension, N is the number of photons, and $\delta_{x,y}$ is the Kronecker delta function. These matrices can be constructed using the special unitary SU(D) generators (of which there are $D^2 - 1$), along with the identity matrix, through all possible tensor product combinations[25]. See below for the orthogonal matrices of the example case.

6. Reconstruct the density matrix, ρ, via the following relationships,

$$\rho = C^{-1}\sum_v M_v n_v$$

$$M_v = \sum_x \Gamma_x (B^{-1})_{x,v}$$

$$B_{x,y} = \langle\psi_x|\Gamma_y|\psi_x\rangle$$

$$C = \sum_v n_v, \text{ for } Tr(M_v) = 1$$

where n_v is the photon counts for the v-th projection vector, $|\psi_x\rangle$ are the projection vectors (see next step), where M_v and B are calculated according to the equation definition.

NOTE: Projection wavevectors for the example case are,

$$|\psi\rangle_1 = \frac{1}{\sqrt{2}}(|\bar{k}\rangle + |\bar{k}+1\rangle) \quad |\psi\rangle_2 = \frac{1}{\sqrt{2}}(|\bar{k}\rangle + |\bar{k}+2\rangle)$$

$$|\psi\rangle_3 = \frac{1}{\sqrt{2}}(|\bar{k}+1\rangle + |\bar{k}+2\rangle)$$

$$|\psi\rangle_4 = \frac{1}{\sqrt{2}}\left(e^{\frac{2\pi i}{3}}|\bar{k}\rangle + e^{\frac{-2\pi i}{3}}|\bar{k}+1\rangle\right)$$

$$|\psi\rangle_5 = \frac{1}{\sqrt{2}}\left(e^{\frac{-2\pi i}{3}}|\bar{k}\rangle + e^{\frac{2\pi i}{3}}|\bar{k}+1\rangle\right)$$
$$|\psi\rangle_6 = \frac{1}{\sqrt{2}}\left(e^{\frac{2\pi i}{3}}|\bar{k}\rangle + e^{\frac{-2\pi i}{3}}|\bar{k}+2\rangle\right)$$
$$|\psi\rangle_7 = \frac{1}{\sqrt{2}}\left(e^{\frac{-2\pi i}{3}}|\bar{k}\rangle + e^{\frac{2\pi i}{3}}|\bar{k}+2\rangle\right)$$
$$|\psi\rangle_8 = \frac{1}{\sqrt{2}}\left(e^{\frac{2\pi i}{3}}|\bar{k}+1\rangle + e^{\frac{-2\pi i}{3}}|\bar{k}+2\rangle\right)$$
$$|\psi\rangle_9 = \frac{1}{\sqrt{2}}\left(e^{\frac{-2\pi i}{3}}|\bar{k}+1\rangle + e^{\frac{2\pi i}{3}}|\bar{k}+2\rangle\right)$$

Experimentally, these wavevectors are realized by imparting the appropriate phase shift on each mode via the programmable filter. Refer to previous publication[25] for discussion on projection vectors. The orthogonal set of matrices, $\{\Gamma\}$ for the example case are chosen first using the SU(3) generators along with the identity matrix,

$$\lambda_1 = \begin{pmatrix} 1 & 0 & 0 \\ 0 & 1 & 0 \\ 0 & 0 & 1 \end{pmatrix}$$
$$\lambda_2 = \begin{pmatrix} 0 & 1 & 0 \\ 1 & 0 & 0 \\ 0 & 0 & 0 \end{pmatrix}$$
$$\lambda_3 = \begin{pmatrix} 0 & -i & 0 \\ i & 0 & 0 \\ 0 & 0 & 0 \end{pmatrix}$$
$$\lambda_4 = \begin{pmatrix} 1 & 0 & 0 \\ 0 & -1 & 0 \\ 0 & 0 & 0 \end{pmatrix}$$
$$\lambda_5 = \begin{pmatrix} 0 & 0 & 1 \\ 0 & 0 & 0 \\ 1 & 0 & 0 \end{pmatrix}$$
$$\lambda_6 = \begin{pmatrix} 0 & 0 & -i \\ 0 & 0 & 0 \\ i & 0 & 0 \end{pmatrix}$$
$$\lambda_7 = \begin{pmatrix} 0 & 0 & 0 \\ 0 & 0 & 1 \\ 0 & 1 & 0 \end{pmatrix}$$
$$\lambda_8 = \begin{pmatrix} 0 & 0 & 0 \\ 0 & 0 & -i \\ 0 & i & 0 \end{pmatrix}$$
$$\lambda_9 = \frac{1}{\sqrt{3}}\begin{pmatrix} 1 & 0 & 0 \\ 0 & 1 & 0 \\ 0 & 0 & -2 \end{pmatrix}$$

and are computed as,

$$\Gamma_x = \lambda_i \otimes \lambda_j$$

7. For a more in-depth discussion of high-dimensional state reconstruction, refer to reference 25 [25].

Representative Results

The outlined scheme for the generation and control of high-dimensional frequency-bin states (based on the excitation of nonlinear micro-cavities, **Figure 1**) is shown in **Figure 2**. This setup uses standard telecommunications components and is highly flexible in the photon production rate and the processing operations applied. **Figure 3** shows the characterization of the generation scheme through the coincidence rate and CAR as function of the repetition rate, demonstrating that the production of photon pairs can be increased without decreasing the CAR. In the control section, programmable filters and phase modulators (**Figure 4A**) allow coherent control of the photon wavefunctions. Such a control scheme is used to perform quantum state tomography of a $D = 3$, two-photon system to reconstruct the state density matrix, as shown in **Figure 4B**. The results demonstrate excellent agreement between the measured and maximally entangled states, with an achieved fidelity of 80.9%.

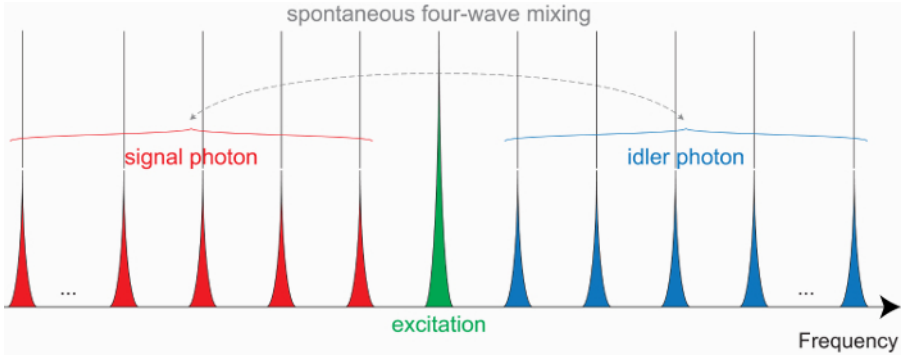

Figure 1: Pulsed quantum frequency comb generation. A pulsed field excites a single nonlinear micro-cavity resonance (green). Spontaneous four-wave mixing mediates the annihilation of two photons from the excitation spectral-mode and the generation of two daughter photons, called signal and idler (red and blue), spectrally symmetric to the excitation. The photon pair is also in a quantum superposition of the frequency modes defined by the resonances, such that in the eigenbasis defined by the state Hamiltonian, the wavefunction is represented by a normalized sum of the symmetric frequency-mode eigenvectors. Please click here to view a larger version of this figure.

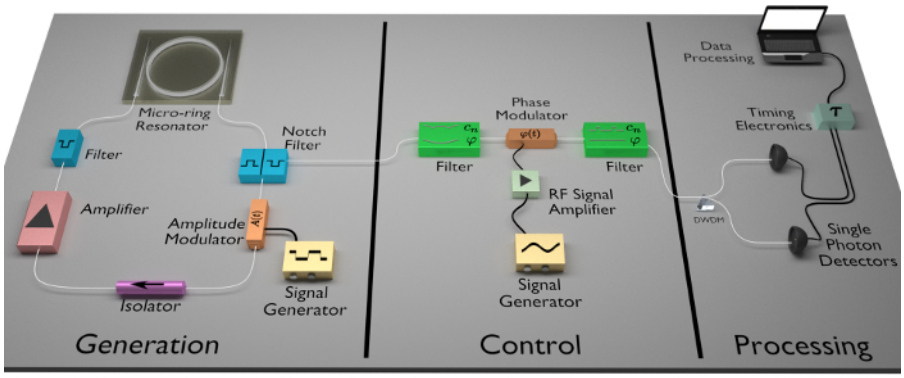

Figure 2: Platform for practical high-dimensional quantum state generation and control. The micro-ring resonator[26,27] is embedded in a larger, external cavity. This external cavity comprises an active electro-optic amplitude modulator driven by a signal generator, an optical gain component, and a narrow band-pass filter, with the latter limiting the circulating excitation pulse to a pass-band corresponding to a single micro-cavity resonance. Quantum frequency combs generated through this scheme (**Figure 1**) are filtered from the excitation field and pass on to the control stage via a notch filter. Here, a concatenation of programmable filters and electro-optic phase modulators (driven by an amplified signal from an RF signal generator) can be used for manipulating the state. In the processing stage, the idler and signal photons are routed to separate single-photon detectors using a DWDM, and the time delay is measured using timing electronics. Please click here to view a larger version of this figure.

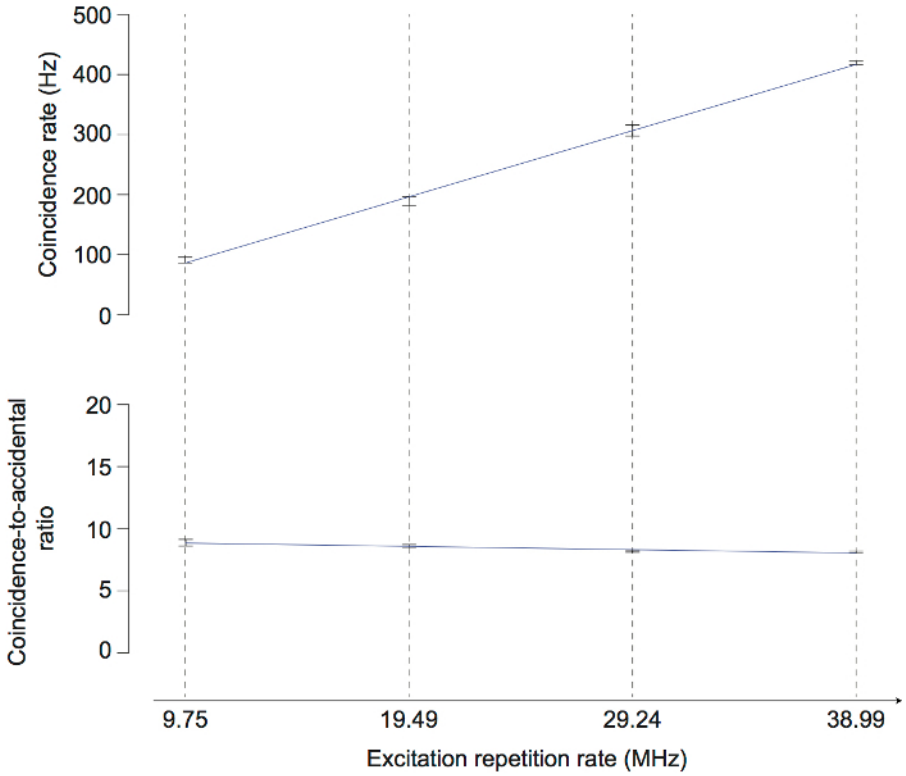

Figure 3: The measured coincidence rate (top) and coincidence-to-accidental ratio (CAR) (bottom) for photon pairs corresponding to the signal-2 and idler-2 frequency modes as a function of increasing repetition rate for harmonically mode-locked pulsed excitation. As the pulse shape and peak powers were maintained for different repetition rates, the coincidence rate was found to grow linearly while the CAR was largely preserved. The slight reduction in CAR and its imperfect linear decrease is imputable to small deviations from the targeted excitation power. The error bars correspond to the standard deviation calculated for five measurements. Please click here to view a larger version of this figure.

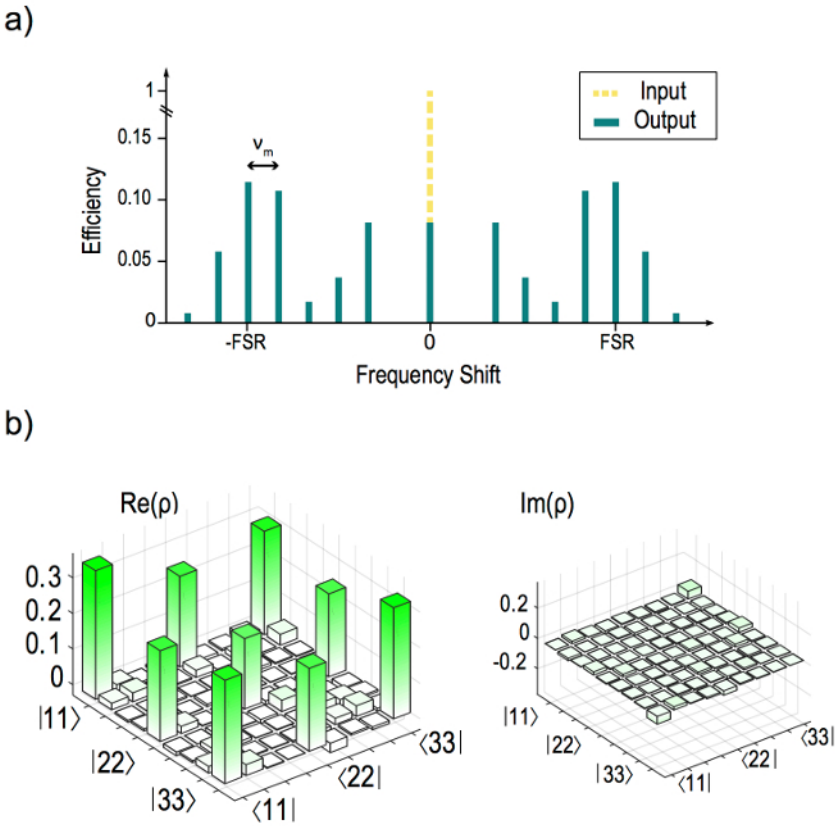

Figure 4: The generation of sidebands via electro-optic phase modulation (top) and example density matrix reconstruction for D = 3 (bottom). (**a**) Frequency sideband generation by an electro-optic modulator as a function of the frequency υ, with side-bands spaced by the frequency of the modulating signal, ν_m. FSR: example free spectral range of a micro-ring resonator. (**b**) Experimental density matrix reconstruction of a D = 3 frequency-bin entangled two-photon state (real and imaginary parts on the left and right, respectively). Please click here to view a larger version of this figure.

Discussion

The optical frequency-domain, via QFCs, is advantageous in quantum applications for a host of reasons. Operations are global, acting on all states simultaneously, which results in a design that does not scale in size or complexity as the state dimensionality increases. This is enhanced as the components can be reconfigured on-the-fly without changing the setup and are capable of being integrated on-chip by exploiting existing and/or developing semiconductor and telecommunications infrastructures. The generation techniques could also be adopted for other optical micro-cavities — such as second-order nonlinear micro-cavities[28], micro-disks[29], photonic crystal waveguides[30,31], *etc*.

Advances in the excitation scheme will pave the way for high production rates, necessary for quantum information processing applications. While the production rate of our generation scheme can be increased by mode-locking at higher harmonic frequencies, supermode noise can lead to instabilities at these higher repetition rates. Suppression of this noise could be accomplished with techniques such as cavity length modulation[32,33], nonlinear compensation[34], and high-finesse supermode filtering techniques[35,36].

Improvements in the system will result in even higher photon production rates. The total losses for the control portion was 14.5 dB (1 dB for the notch filter, 4.5 dB for the first programmable filter, 3.5 dB for the phase modulator, and 4.5 dB for the second programmable filter). Production rates could be increased many-fold through realizable reductions in losses – with a readily available improvement of 5 dB by integrating many of the control components used in the setup into a single compact, lower-loss optical chip.

Improved control of the frequency-mode mixing through better targeted side-band creation will provide more efficient gates and higher production rates. As the probability scattering depends on the modulation driving signal (pattern, frequency, and amplitude) and electro-optic modulator specifications, these must be in the realm to effectively overlap modes (generate side-bands) at the desired mixing frequencies — requiring RF (GHz) signal speeds, state-of-the-art voltage amplifiers and low V_π phase modulators.

Current programmable filters are limited in the spectral bandwidth and resolution; the equipment used in the original demonstrations had a bandwidth from 1527.4 nm to 1567.5 nm and a resolution of 12.5 GHz. With a micro-ring FSR of 200 GHz, this programmable filter provides access to 10 signal and 10 idler frequencies. The dimensionality of these quantum states could readily reach values upwards of $D = 100$

(corresponding to as many as 14 qubits) with advances in programmable filter bandwidth/resolution and optical cavity FSR — all without increasing the footprint of the setup.

With the QFC platform outlined here, we demonstrate the generation and control of complex quantum states in a *compact, reconfigurable,* and *practical* way. The highlights of our schemes are the capability for high generation rates of pure single photons and global operation on all states with single components, allowing scalability in the form of mass-produced, low-cost, integrated photonic chips and accessible telecommunications components. Using this QFC platform, significant steps are made towards quantum information processing technologies. Quantum communication at high rates is realizable with multiplexed channels, allowing secure information transfer at very efficient rates, while high-dimensional quantum computing is a developing field that could help overcome the limitations of qubit-based computation[37].

Acknowledgements

We thank R. Helsten for technical insights; P. Kung from QPS Photronics for the help and processing equipment; as well as QuantumOpus and N. Bertone of OptoElectronics Components for their support and for providing us with state-of-the-art photon detection equipment. This work was made possible by the following funding sources: Natural Sciences and Engineering Research Council of Canada (NSERC) (Steacie, Strategic, Discovery, and Acceleration Grants Schemes, Vanier Canada Graduate Scholarships, USRA Scholarship); Mitacs (IT06530) and PBEEE (207748); MESI PSR-SIIRI Initiative; Canada Research Chair Program; Australian Research Council Discovery Projects (DP150104327); European Union's Horizon 2020 research and innovation program under the Marie Sklodowska-Curie grant (656607); CityU SRG-Fd program (7004189); Strategic Priority Research Program of the Chinese Academy of Sciences (XDB24030300); People Programme (Marie Curie Actions) of the European Union's FP7 Programme under REA grant agreement INCIPIT (PIOF-GA-2013-625466); Government of the Russian Federation through the ITMO Fellowship and Professorship Program (Grant 074-U 01); 1000 Talents Sichuan Program (China)

References

1. Kimble, H. J. The quantum internet. *Nature.* **453** (7198), 1023-1030 (2008).
2. Knill, E., Laflamme, R., & Milburn, G. J. A scheme for efficient quantum computation with linear optics. *Nature.* **409** (6816), 46-52 (2001).
3. Israel, Y., Rosen, S., & Silberberg, Y. Supersensitive Polarization Microscopy Using NOON States of Light. *Physical Review Letters.* **112** (10), 103604 (2014).
4. Ladd, T. D., Jelezko, F., Laflamme, R., Nakamura, Y., Monroe, C., & O'Brien, J. L. Quantum Computing. *Nature.* **464** (7285), 45-53 (2010).
5. Schaeff, C., Polster, R., Lapkiewicz, R., Fickler, R., Ramelow, S., & Zeilinger, A. Scalable fiber integrated source for higher-dimensional path-entangled photonic quNits. *Optics Express.* **20** (15), 16145 (2012).
6. Thew, R., Acin, A., Zbinden, H., Gisin, N. Experimental realization of entangled qutrits for quantum communication. *Quantum Information and Computation.* **4** (2), 93 (2004).
7. Pasquazi, A. *et al.* Micro-combs: A novel generation of optical sources. *Physics Reports.* (2017).
8. Caspani, L. *et al.* Multifrequency sources of quantum correlated photon pairs on-chip: a path toward integrated Quantum Frequency Combs. *Nanophotonics.* **5** (2), 351-362 (2016).
9. Kues, M. *et al.* On-chip generation of high-dimensional entangled quantum states and their coherent control. *Nature.* **546** (7660), 622-626 (2017).
10. Olislager, L. *et al.* Frequency-bin entangled photons. *Physical Review A - Atomic, Molecular, and Optical Physics.* **82** (1), 1-7 (2010).
11. Lu, Y. J., Campbell, R. L., & Ou, Z. Y. Mode-Locked Two-Photon States. *Physical Review Letters.* **91** (16), 1636021-1636024 (2003).
12. Reimer, C. *et al.* Integrated frequency comb source of heralded single photons. *Optics Express.* **22** (6), 6535-6546 (2014).
13. Reimer, C. *et al.* Cross-polarized photon-pair generation and bi-chromatically pumped optical parametric oscillation on a chip. *Nature Communications.* **6**, 8236 (2015).
14. Grassani, D. *et al.* Micrometer-scale integrated silicon source of time-energy entangled photons. *Optica.* **2** (2), 88 (2015).
15. Reimer, C. *et al.* Generation of multiphoton entangled quantum states by means of integrated frequency combs. *Science.* **351** (6278), 1176-1180 (2016).
16. Mazeas, F. *et al.* High-quality photonic entanglement for wavelength-multiplexed quantum communication based on a silicon chip. *Optics Express.* **24** (25), 28731 (2016).
17. Imany, P. *et al.* Demonstration of frequency-bin entanglement in an integrated optical microresonator. *Conference on Lasers and Electro-Optics.* **62** (19), JTh5B.3 (2017).
18. Roztocki, P. *et al.* Practical system for the generation of pulsed quantum frequency combs. *Optics Express.* **25** (16), 18940 (2017).
19. Haus, H. A. Mode-locking of lasers. *IEEE Journal on Selected Topics in Quantum Electronics.* **6** (6), 1173-1185 (2000).
20. Walmsley, I., & Raymer, M. Toward Quantum-Information Processing with Photons. *Science.* **307** (March), 1733-1735 (2005).
21. Olislager, L., Woodhead, E., Phan Huy, K., Merolla, J. M., Emplit, P., & Massar, S. Creating and manipulating entangled optical qubits in the frequency domain. *Physical Review A - Atomic, Molecular, and Optical Physics.* **89** (5), 1-8 (2014).
22. *Finisar WaveShaper Software.* at <https://www.finisar.com/optical-instrumentation> (2018).
23. Capmany, J., & Fernández-Pousa, C. R. Quantum model for electro-optical phase modulation. *Journal of the Optical Society of America B.* **27** (6), A119 (2010).
24. Stocklin, F. *Relative sideband amplitudes versus modulation index for common functions using frequency and phase modulation.* (1973).
25. Thew, R. T., Nemoto, K., White, A. G., & Munro, W. J. *Qudit quantum-state tomography.* 1-6 (2002).
26. Moss, D. J., Morandotti, R., Gaeta, A. L., & Lipson, M. New CMOS-compatible platforms based on silicon nitride and Hydex for nonlinear optics. *Nature Photonics.* **7** (8), 597-607 (2013).
27. Caspani, L. *et al.* Integrated sources of photon quantum states based on nonlinear optics. *Light: Science & Applications.* **6** (11), e17100 (2017).
28. Guo, X., Zou, C., Schuck, C., Jung, H., Cheng, R., & Tang, H. X. Parametric down-conversion photon-pair source on a nanophotonic chip. *Light: Science & Applications.* **6** (5), e16249 (2016).
29. Jiang, W. C., Lu, X., Zhang, J., Painter, O., & Lin, Q. Silicon-chip source of bright photon pairs. *Optics Express.* **23** (16), 20884 (2015).

30. Xiong, C. *et al.* Slow-light enhanced correlated photon pair generation in a silicon photonic crystal waveguide. *Optics Letters.* **36** (17), 3413 (2011).
31. Kumar, R., Ong, J. R., Savanier, M., & Mookherjea, S. Controlling the spectrum of photons generated on a silicon nanophotonic chip. *Nature communications.* **5**, 5489 (2014).
32. Shan, X., Cleland, D., & Ellis, A. Stabilising Er fibre soliton laser with pulse phase locking. *Electronics Letters.* **28** (2), 182 (1992).
33. Shan, X., & Spirit, D. M. Novel method to suppress noise in harmonically modelocked erbium fibre lasers. *Electronics Letters.* **29** (11), 979-981 (1993).
34. Thoen, E. R., Grein, M. E., Koontz, E. M., Ippen, E. P., Haus, H. A., & Kolodziejski, L. A. Stabilization of an active harmonically mode-locked fiber laser using two-photon absorption. *Optics Letters.* **25** (13), 948 (2000).
35. Harvey, G. T., & Mollenauer, L. F. Harmonically mode-locked fiber ring laser with an internal Fabry-Perot stabilizer for soliton transmission. *Optics Letters.* **18** (2), 107 (1993).
36. Gee, S., Quinlan, F., Ozharar, S., & Delfyett, P. J. Simultaneous optical comb frequency stabilization and super-mode noise suppression of harmonically mode-locked semiconductor ring laser using an intracavity etalon. *IEEE Photonics Technology Letters.* **17** (1), 199-201 (2005).
37. Babazadeh, A. *et al.* High-Dimensional Single-Photon Quantum Gates: Concepts and Experiments. *Physical Review Letters.* **119** (18), 1-6 (2017).

